NASA Wind Satellite (1994)

Adam Szabo

Contents

Abstract

The NASA Wind spacecraft, launched in November 1994, provides comprehensive and continuous in situ solar wind measurements while orbiting the Sun–Earth first Lagrange point upstream of Earth. The spacecraft has a full complement of instruments to measure the local magnetic and electric fields and thermal solar wind and high-energy charged particles at unprecedented high time resolutions. After nearly 20 years of operation, the spacecraft and most instruments are fully operational, and Wind is expected to remain in service for many years to come. While Wind provides real-time solar wind measurements for only about 2 h every day – thus it is not considered an operational space weather monitor – the high-quality and continuous Wind observations have been critical in developing current space weather forecasting techniques. In particular, Wind observations led to better understanding of the propagation and evolution

A. Szabo (✉)
Heliospheric Physics Laboratory, NASA Goddard Space Flight Center, Greenbelt, MD, USA
e-mail: Adam.Szabo@nasa.gov

J.N. Pelton, F. Allahdadi (eds.), *Handbook of Cosmic Hazards and Planetary Defense*,
DOI 10.1007/978-3-319-03952-7_13

of coronal mass ejections quantifying their distortions and deflections. Wind radio science results significantly added to the understanding of the inner heliospheric propagation of interplanetary shocks and high time resolution field and particle measurements revealed the mechanisms of how these shocks and magnetic reconnection can accelerate charged particles to very high and harmful energies. Wind is expected to continue its contribution to the development of future space weather forecasting capabilities as its measurements near two complete 11-year solar cycles allowing the identification of long-term trends.

Keywords

Wind spacecraft • Solar wind • Interplanetary magnetic field • First Lagrange point • Coronal mass ejections • Magnetic cloud • Magnetic flux rope • Interplanetary shocks • Solar energetic particles • Solar flares • Magnetic reconnection • Heliosphere • Magnetosphere • Bow shock • Space weather • Type II radio burst • Solar cycle

Introduction

NASA launched the Wind spacecraft in November 1994 to the Earth's first Lagrange point (L1) as the interplanetary component of the Global Geospace Science (GGS) program within the International Solar Terrestrial Physics (ISTP) program. An orbit around the L1 point, upstream of Earth, toward the Sun, and four times further away than the Moon, provides a unique opportunity to observe the undisturbed solar wind before it impinges on the Earth's magnetosphere (see Fig. 1). The original science objectives of the Wind mission were (1) to make accurate in situ measurements of interplanetary conditions upstream of the magnetosphere to complement measurements made inside the magnetosphere by the Polar and Geotail spacecraft, other elements of the GGS program, and (2) to remotely sense interplanetary disturbances for possible future predictive purposes.

The spin-stabilized Wind spacecraft – spin axis aligned with ecliptic south – carries eight instrument suites that provide comprehensive and continuous measurements of the thermal solar wind to solar energetic particles, quasi-static magnetic and electric fields to high-frequency radio waves, and γ-rays. After nearly 20 years of operation, Wind is still returning all of these measurements that became essential for solar wind studies and serves as 1 AU baseline for deep space (inner and outer heliospheric) missions and as a reliable input for magnetospheric investigations long after the termination of the GGS and ISTP programs. The sections below review the rich contributions of the Wind mission to the subject of understanding the structure and propagation of coronal mass ejections (CMEs), interplanetary shocks, and corotating interaction regions (CIRs) and to the acceleration and transport of solar energetic particles (SEPs).

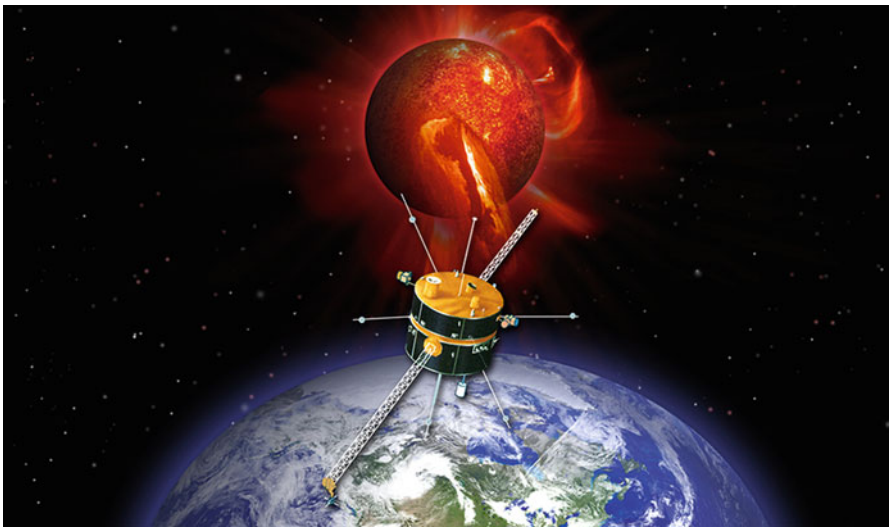

Fig. 1 Artist depiction of the Wind spacecraft orbiting the Sun–Earth first Lagrange point observing the incoming solar wind. The two long booms hold the magnetometers and the four wire antennas, and two axial booms measure the electric magnetic field waves. The other instruments are housed inside of the spacecraft body

The Orbit of the Wind Spacecraft

The first Sun–Earth Lagrange point, on the Sun–Earth line between the two objects, marks the position where the combined gravitational pull of the Sun and Earth provides precisely the centripetal force required to orbit with them. Thus a satellite at L1 will have a heliocentric orbit with a slightly smaller orbital radius but the same angular speed as Earth. In effect, the spacecraft will appear from Earth to be motionless, hovering 1.5 million km (or four times further than the Moon) upstream of Earth. In practice, the L1 Lagrange point – named after the eighteenth-century Italian mathematician and astronomer Joseph-Louis Lagrange – is not stable due to the eccentricity of the Earth's orbit and other forces. Neither is it desirable to park a spacecraft exactly on the Sun–Earth line, making communication with it difficult due to intense radio emissions from the Sun. Fortunately, there exists a class of semi-periodic – not exactly repeating but bounded by a box – orbit around L1, called a Lissajous orbit that keeps the spacecraft outside of a 3–4° solar radio exclusion region, yet keeps it continuously upwind from Earth with minimal orbit correction requirements. The Wind spacecraft was only the second mission to take advantage of this kind of an orbit after the very successful ISEE-3 mission (1978–1982).

After a number of petal orbits and a double lunar swingby, Wind reached L1 in 1996. However, it did not stay in the vicinity of L1 for long as it was soon joined

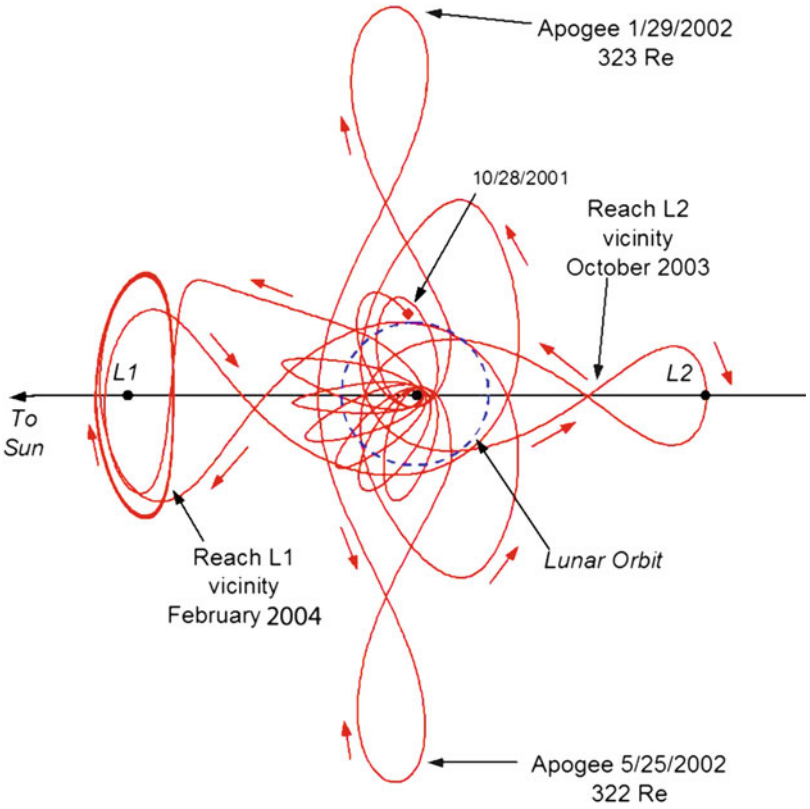

Fig. 2 The complex orbit of the Wind spacecraft between 2001 and 2004 in ecliptic coordinates. The plot is centered on Earth with the Sun to the left. The lunar orbit is marked by *blue dashed lines*

there by the Advanced Composition Explorer (ACE), another NASA solar wind mission. With Wind's very large fuel reserve and with its spin axis perpendicular to the ecliptic (ACE's spin axis is pointing at the Sun in constant need of realignment as the spacecraft is orbiting around the Sun), it was decided to relocate the Wind spacecraft to various, scientifically advantageous locations. In 1999 Wind executed a number of magnetospheric petal orbits that took it to the rarely sampled geomagnetic high latitudes. Between 2000 and 2002, Wind moved further and further away from the Sun–Earth line (and from ACE) reaching 2.3 million km to the side in a distant prograde orbit (see Fig. 2). Finally in 2003 it completed a second Lagrange (L2) point campaign, taking the spacecraft more than 1.5 million km downstream of Earth and ~3 million km downstream of ACE, to investigate solar wind evolution and magnetotail phenomena. Since 2004 Wind has remained at L1 in a Lissajous orbit bounded by +/− 600,000 km perpendicular to the Sun–Earth line in the ecliptic and +/− 120,000 km perpendicular to the ecliptic. It should be noted that

this is a very large orbit as the maximum radius of the Earth's geomagnetic tail is only around 150,000 km. Thus, propagating solar wind observations to Earth is a nontrivial task. The Wind spacecraft has enough fuel left to maintain its current orbit for almost 60 more years.

Spacecraft Design

Wind was designed and manufactured by Martin Marietta of Astro Space Division in East Windsor, New Jersey. The satellite is a spin-stabilized cylindrical satellite with a diameter of 2.4 m and a height of 1.8 m (see Fig. 1). It has an approximately 3 s rotation period. With its 1,150 kg mass, two 50 m and two 7.5 m wire antennas, and two 12 m lanyard booms, the spacecraft has an immense angular momentum, rendering it an extremely stable platform, ideal for long-term, continuous solar wind measurements. Wind has body-mounted solar panels, only some of which see the Sun at any given time. At the beginning of the mission, the solar panels generated 472 W of power with a 100 W margin that allowed for ample aging degradation. The spacecraft will be able to operate all its subsystems simultaneously at least for the next 10 years. The instruments record their measurements to a tape deck, from which it is read back at high speed, nominally once a day for 2 h. This downlink telemetry takes place via an S-band system to the NASA Deep Space Network (DSN) at 64 kbps.

Instrumentation

The Wind spacecraft carries eight instrument suites that provide comprehensive measurements of the solar wind thermal particles to solar energetic particles, quasi-static electromagnetic fields to high-frequency radio waves, and γ-rays. Table 1 lists all of these instrument suites and their capabilities and current status. Wind's complement of instruments was optimized for studies of solar wind plasma, interplanetary magnetic field, radio and plasma waves, and low energetic particles. The instrument suite is not equivalent to that on ACE, rather the two missions complement each other. Wind is the only near-Earth spacecraft capable of making remote radio wave measurements and hence tracking interplanetary shocks from the Sun to Earth. Moreover, Wind provides solar wind measurements with an unprecedented accuracy. It measures solar wind particle densities with three different instruments (SWE, 3DP, and WAVES) relying on different measurement techniques. Intercalibrating these three observations yields an absolute accuracy of better than 1 %. Wind also provides the highest time resolution measurements in the near-Earth environment (11 vectors/s for magnetic field and a 3 s cadence for plasma observations). Finally, Wind has accumulated solar wind observations for nearly two complete solar cycles (a solar magnetic cycle is ~11 years long). Thus, Wind is ideally positioned to study solar wind transients that have adverse space weather effects.

Table 1 The Wind spacecraft instrument suite and its current status

Instrument	Description	Status
Magnetic field investigation (MFI)	Slowly varying vector magnetic fields (0–64,000 nT, 0–5.5 Hz)	Fully operational
Solar wind experiment (SWE)	Density, velocity, and temperature of solar wind thermal ions (150 eV–8 keV) and electrons (5 eV–24.8 keV)	Ion sensors fully operational. Electron measurements limited to energies below 5 keV
3D plasma experiment (3DP)	Full 3D distribution function of solar wind ions and electrons (3 eV–30 keV)	Fully operational
	Energetic ions (25 keV–11 MeV) and energetic electrons (20 keV–1 MeV)	
Radio and plasma wave experiment (WAVES)	Electric and magnetic field waves (0.3 Hz–14 MHz)	Fully operational
Suprathermal particle experiment (SMS)	Suprathermal ions (H–Fe) in the energy range (0.5–226 keV/e)	The low-energy SWICS sensor is not operational
		The STICS and MASS sensor fully operational
High-energy particle experiment (EPACT)	Energetic particles (0.04–500 MeV/nuc)	Only the lower-energy detectors LEMT and STEP are operational (0.04–10 MeV/nuc)
KONUS	High-time resolution gamma-ray detector	Fully operational
Transient gamma-ray spectrometer (TGRS)	High spectral resolution gamma-ray detector in the energy range 15 keV–10 MeV	All the coolants used up. Instrument turned off

The Ambient Solar Wind

The visible surface of the Sun, the photosphere, is at an effective temperature of 5,800 K, and it continuously emits charged particles called the solar wind. This solar wind – composed mostly of protons and electrons, 4 % (by number) helium nuclei (alpha particles), and traces of heavier ions – is heated to over a million degrees of Kelvin in the solar corona, 2,000 km above the photosphere. The solar wind particles are not only heated but also accelerated to 200–800 km/s of speed dragging with them the magnetic field of the Sun. This enormous speed (a fast bullet can reach 1 km/s and the fastest spacecraft launch ever was 16.26 km/s for New Horizon, a mission to Pluto) is faster than information can travel in this medium. Thus, as the solar wind flow approaches obstacles (like planets), information cannot flow upstream fast enough to divert the particles and they pile up

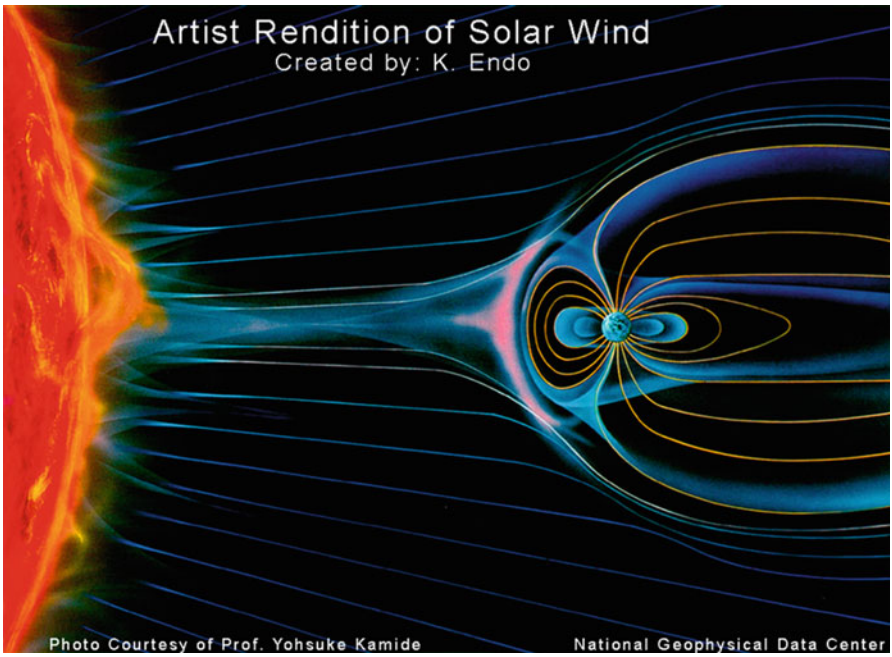

Fig. 3 Artist rendition of the solar wind flowing around the Earth's magnetosphere. The *blue lines* represent plasma flow directions. The *yellow lines* connected to Earth are magnetic field lines (Courtesy of K. Endo and Prof. Yohsuke Kamide)

forming a shock wave, not unlike a sonic boom in front of a supersonic airplane. In the case of Earth, this shock wave, called the bow shock, forms around 100,000 km, or 15 Earth radii upstream, toward the Sun. At this boundary, the solar wind particles abruptly slow down and change direction to flow around the planet (see Fig. 3). The Earth is a magnetized planet; thus, the obstacle that the solar wind plasma reacts to is not the surface of the planet, but its magnetic field that charge particles cannot cross. In turn, the shocked solar wind flowing around the planet compresses the Earth's magnetic field into a large bubble, called the magnetosphere, till an energy balance is reached between the kinetic energy of the incoming solar wind flow and the magnetic energy of the magnetosphere. This energy balance boundary, the magnetopause, is just above 60,000 km at the subsolar point. Solar wind particles cannot cross through the magnetopause and thus cannot reach the surface of the Earth except near the magnetic poles where the vertically oriented magnetic field lines can exert only minimal pressure. But even at the magnetic poles, the extremely low-density solar wind of 10 particles per cubic centimeter (compared to 6×10^{23} particles/cm^3 of the surface atmosphere) is quickly absorbed by the neutral atmosphere posing no danger to humankind. Therefore, it is not the ambient solar wind that represents a cosmic hazard. Rather, the large transients embedded in it that cause rapid variations in the compression of the magnetosphere are the chief culprit. These transients are discussed in the next sections.

Coronal Mass Ejections (CMEs)

Coronal mass ejections (CMEs) are the most hazardous solar transients for man-made systems like electric power grids or oil pipelines. Sometimes as frequently as several times a day, but at least once every couple of weeks, the Sun ejects an extra dose of charged particles. Most of these CMEs originate from active regions on the Sun's surface, such as groupings of sunspots associated with frequent solar flares. These regions have closed magnetic field lines, in which the magnetic field strength is large enough to contain the plasma. These field lines must be broken or weakened – probably via magnetic reconnection – for the plasma to escape from the Sun. The released CMEs have a wide range of velocities between 20 and 3,200 km/s. The slower ones are accelerated and the fast ones are decelerated by the solar wind so that by 1 AU the range of their speeds is much smaller. It takes between 1 and 3 days for them to reach Earth. Even though the average ejected mass in a CME is a staggering 1.6×10^{12} kg, it is the embedded magnetic field that is responsible for most of the geomagnetic response. CMEs expand their volume faster than the ambient solar wind – the solar wind expands nearly spherically resulting in a $1/r^2$ reduction in the solar wind density – thus by 1 AU their internal particle density is typically comparable or smaller than that of the ambient solar wind. However, the embedded magnetic field strength is several times – up to an order of magnitude – larger than the 1 AU interplanetary magnetic field. This extra field pressure compresses the Earth's magnetosphere. Moreover, the CME internal magnetic field often takes a helical flux rope geometry – referred to as magnetic clouds (MCs) – with prolonged periods of large, ecliptic southward-pointing components. When squeezed against the northward-oriented subsolar magnetic field of Earth, they reconnect (cancel), weakening the internal magnetic pressure in the magnetosphere and thus rapidly further compressing the surface magnetic fields. These rapid magnetic fluctuations generate current in all conducting materials like a giant alternator. The amount of excess current generated is proportional to the length of the conducting material. Thus, electric power grid lines and oil pipelines that can span multiple states will experience the most excess current flows overloading transformers and weakening welding lines. Therefore, it is imperative to develop a forecasting capability that can accurately predict the arrival of the largest of these CMEs.

Current space weather monitoring spacecraft at L1 (like the ACE spacecraft or the future Deep Space Climate Observatory, DSCOVR) provide 15–45 min of warning time by measuring the local or in situ signatures of an incoming CME. To expand the forecasting interval to 1–3 days, the initiation of CMEs near the Sun has to be observed remotely and the propagation of these CMEs to 1 AU accurately modeled. The primary contribution of the Wind spacecraft to CME forecasting is in the area of developing these CME propagation and evolution models.

While there is a very good correlation between CMEs at 1 AU and coronal CMEs (Gopalswamy et al. 2000) observed by white light coronagraphs, the reverse is not true. Even when limiting the study to only front-side full-halo CMEs, Michalek et al. (2004) found that only 83 out of 123 solar events had discernible

1 AU counterparts. What happened to a third of the CMEs? Were they processed by the solar wind so much that they became indistinguishable from the background flow? Or were they deflected by an unusual amount so that they missed Earth? Measurements made by Wind and other spacecraft give us some clues.

Not every visible light CME observed near the Sun will maintain its dangerous magnetic flux rope topology by the time it reaches 1 AU. These irregular ejecta can still be identified by the Wind spacecraft by counter-streaming heat flux electrons, electrons with slightly more energy than the average solar wind component. These heat flux electrons travel faster than the solar wind but follow very precisely the interplanetary magnetic field lines. Thus, no matter what geometrical shape the CME takes at 1 AU, as long as both foot points of the internal magnetic field lines are still encored to the Sun, heat flux electrons will travel in both directions clearly delineating the CME from the ambient solar wind where only one end of the field lines is connected to the Sun, and thus heat flux electrons flow only in one direction. By identifying these irregular ejecta, the Wind measurements clearly identify that these CMEs dissipated harmlessly. What internal or external condition determines whether a CME dissipates or not is the subject of ongoing research.

The most harmful CMEs preserve their magnetic flux rope configuration to 1 AU. However, even these powerful transients can be distorted by the ambient solar wind, changing their magnetic impact on the Earth system. Traditionally, CMEs are drawn as large horseshoe-shaped structures with embedded helical magnetic fields, with the field wound up much more near the surface and axial near the center (see Fig. 4). In contrast, STEREO white light images appear to show significant pancaking, not unlike some magnetohydrodynamic numerical simulations suggest (see Fig. 5). However, Wind magnetic field observations can be fitted rather well with simple circular cross-section flux rope models. In fact, even simultaneous three-spacecraft 3D reconstruction of the CME internal magnetic field lines, using magnetic field measurements from Wind and the two STEREO spacecraft, shows very little geometrical distortions. A recent, multi-spacecraft study has solved this dilemma by demonstrating that the white light images suffer from projection effects that make the CMEs look much more elongated than they are (Nieves-Chinchilla et al. 2012). This is a significant result, as it shows that those CMEs that do not dissipate will likely retain their near-circular cross section allowing more reliable forecasting.

The shape of CMEs in the third dimension, along their symmetry axis, is much more difficult to observe at 1 AU. There are only a handful of fortuitous in situ observations of the same CME by multiple, well-separated spacecraft, as the CME has to lie nearly perfectly in the ecliptic and propagate toward Earth, a situation that happens only very rarely. But for these few cases, it has been shown that CMEs can twist and change the direction of their propagation significantly before reaching Earth (Möstl et al. 2012). Particularly during maximum solar activity years, when multiple CMEs are ejected in close proximity to each other, CMEs can interact with each other significantly deflecting their propagation. While multi-spacecraft observations cannot be relied on as a space weather forecasting technique, these cases serve as benchmark events for numerical and empirical space weather prediction models.

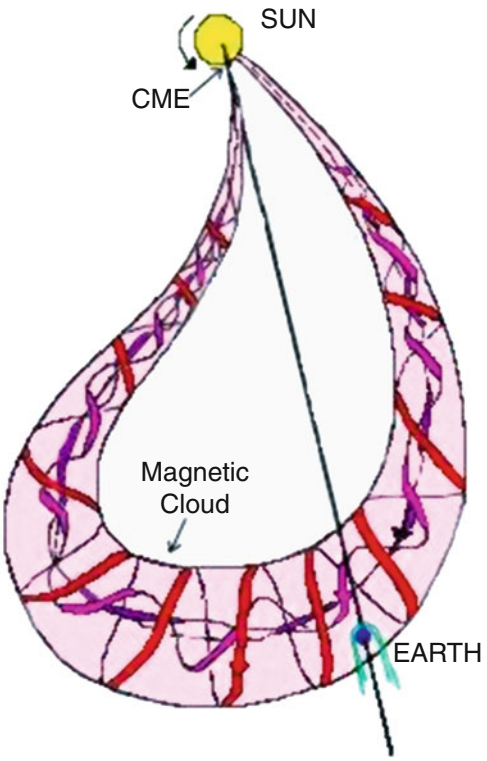

Fig. 4 The idealized horseshoe shape of a CME magnetic flux rope. The internal magnetic field lines follow a helical direction with less and less winding toward the center of the structure (After Marubashi 1997)

Further insight into the global geometry of CMEs can be obtained using energetic particles as magnetic field line tracers. Solar flares, sudden releases of very energetic particles in the solar atmosphere, spew out simultaneously charged particles at different energies, thus speeds. If the flare happens at the foot point of the CME, the released energetic particles will follow the internal magnetic field lines of the CME with the more energetic and faster particles reaching the 1 AU observer – in this case the Wind spacecraft 3DP instrument – before the slower ones. The start of the energetic electrons is marked by a type III radio burst with the radio signal traveling in a straight line at the speed of light and measured by the Wind spacecraft radio antennas. Using these time differences, the length of the magnetic field lines from the Sun to 1 AU can be computed with great accuracy and compared to the predictions of helical flux rope geometry models. Such studies resulted in good agreements deep inside the CME, but not near the boundary (Kahler et al. 2011). This implies that, in addition to deflection and distortion, CME surface magnetic fields also reconnect with the ambient interplanetary magnetic fields, in effect peeling away one layer at a time of their structure.

Thus, wind measurements, together with other spacecraft, have enabled the identification of the key processes of CME interplanetary propagation and evolution. It remains to distill these results into a space weather prediction model.

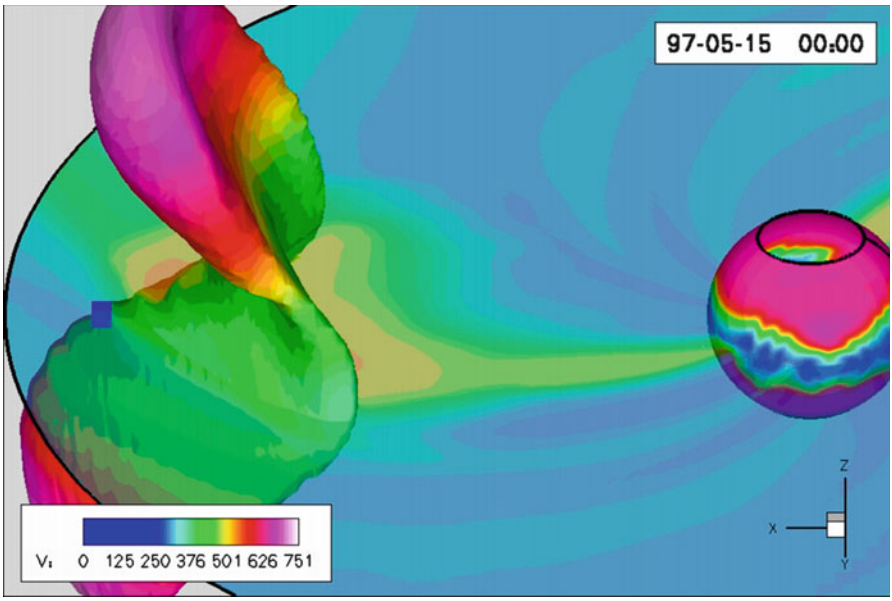

Fig. 5 Global magnetohydrodynamic simulation of the evolution of a CME in the inner heliosphere. The injected CME is shown as an iso-surface at 25 % of maximum density. The color scale shows the flow velocities on the iso-surface and from the solar source surface. The *small blue box* toward the *left* of the figure shows the Earth's position (Odstrcil et al. 2004)

Interplanetary Shocks

Besides CMEs any sudden pressure increase in the solar wind can compress the Earth's magnetic field with negative consequences. Especially effective are interplanetary shocks where fast-moving solar wind streams overtake slowly moving parcels with a speed difference greater than any of the plasma wave mode speeds. At shocks, the plasma of the fast-moving stream piles up against the slow stream resulting in a density jump of up to a factor of four in a few seconds. Fast-moving CMEs can act like fast-moving pistons driving an interplanetary shock in front of them.

Another source of interplanetary shocks is corotating interaction regions (CIRs) where a stream of fast solar wind overtakes a parcel of slow solar wind that was emitted from the Sun at an earlier time. During solar activity minimum years on the Sun, when the solar magnetic field is nearly dipolar, the Sun emits fast (~800 km/s) solar wind at high latitudes and much slower winds (300–450 km/s) near the magnetic equator (see Fig. 6). Since the magnetic dipole axis of the Sun is tilted with respect to its rotation axis, as the Sun rotates, fast streams are emitted behind slow parcels near the fast–slow wind boundary. These fast streams running into slow ones form CIRs, often steepening into fully formed shocks by 1 AU.

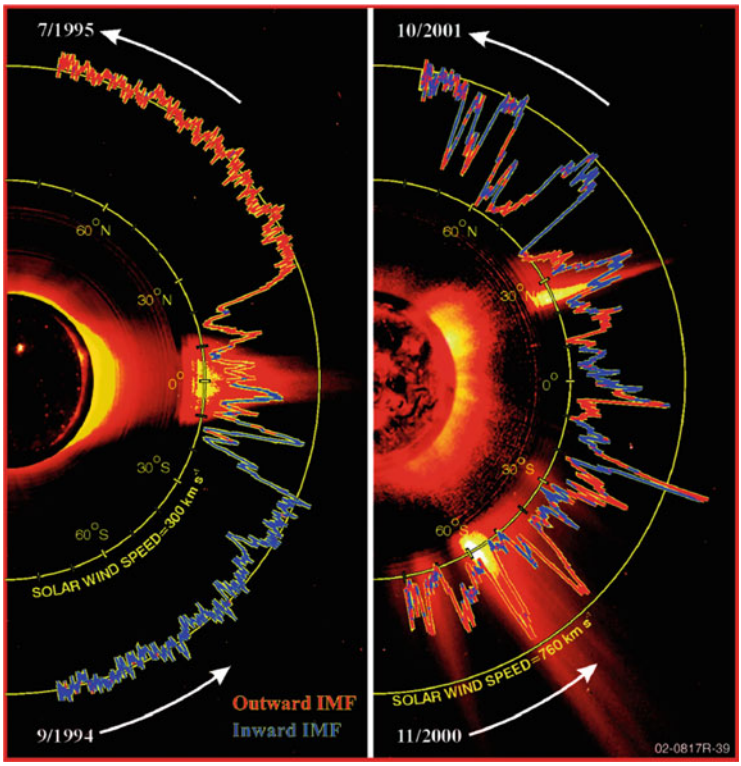

Fig. 6 Solar wind observations collected by the Ulysses spacecraft during two separate polar orbits of the Sun, 6 years apart at nearly opposite times in the 11-year solar cycle. Near solar minimum (*left*), the slow solar wind is limited to low latitudes. Near solar maximum (*right*), the fast and slow streams are more intermingled (Courtesy of Southwest Research Institute and the Ulysses/SWOOPS team)

During solar maximum years, the picture becomes much more complicated with fast and slow streams intermingling at all latitudes (see Fig. 6).

Current global heliospheric models can accurately predict the arrival of CIR compression regions at Earth with about 3 days of warning time. Forecasting the arrival of CME-driven shocks is much more complicated. Moreover, unlike CIR shocks that are almost always aligned with the local Parker spiral direction (about 45° relative to the Sun–Earth line at 1 AU), CME-driven shocks can have almost any orientation. This introduces a large uncertainty in the predicted arrival times at Earth even from the L1 monitors (like ACE). As mentioned above, the L1 monitors orbit the L1 point that takes them several times further to the side than the diameter of the magnetosphere. For nonradially aligned structures, this requires the determination of the orientation of these fronts. Local surface normals can be computed based on the in situ measurements; however, these directions reflect the small ripples on the shock surfaces, not their global orientation. Multi-spacecraft

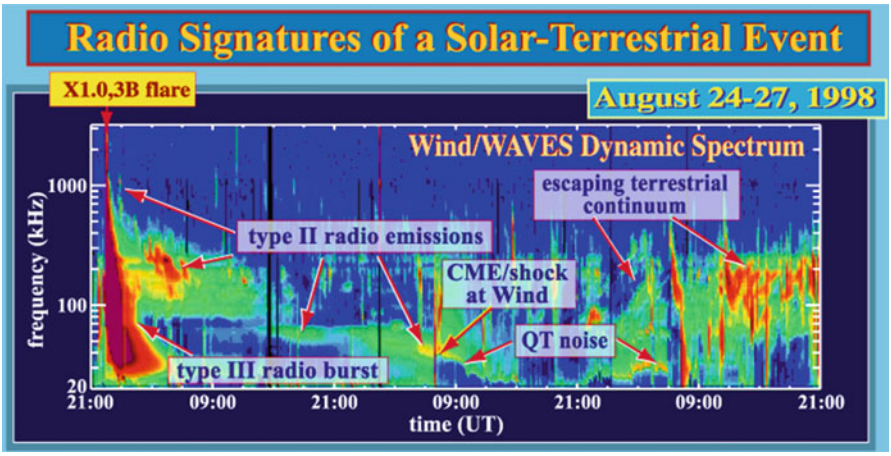

Fig. 7 Radio spectrogram of the August 24–27, 1998, CME observed by the Wind spacecraft. *Red color* represents high-intensity emissions. Shortly after 21:00 UT on August 24, the bright feature covering the full frequency range is a type III burst associated with a solar flare. The slowly descending feature is the type II burst related to the outward-propagating CME-driven shock. The shock reaches the Wind and Earth just before 9:00 on August 26 (Courtesy of the Wind/WAVES team)

techniques have been successfully employed, combining measurements from Wind, ACE, SOHO, and the Genesis spacecraft, to reduce the prediction uncertainty from 10–15 min to 1–2 min. However, this technique does require four simultaneous real-time solar wind monitors to operate upstream of Earth.

Fortunately, interplanetary shocks are strong radio emitters. The shocks accelerate electrons locally. The faster electrons race ahead, creating a plasma instability that through nonlinear wave–wave interactions produce the so-called type II radio emissions at the local electron plasma frequency and at its second harmonic. As the shock propagates away from the Sun and the local solar wind density drops, the frequency of these type II radio bursts also decreases. The radio receivers on-board the Wind spacecraft observe these radio signals (see Fig. 7) and thus are able to track shocks from the Sun all the way to 1 AU. Moreover, since the Wind spacecraft rotates in the ecliptic plane, it can determine the direction from which the signal is emanating (like a rotating radar dish). Combining the Wind radio measurements with those on STEREO, the signal can even be precisely triangulated to yield an exact location in space for each radio burst. The only unknown in this observational scheme is the precise radial solar wind density profile. Using global magnetohydrodynamic solar wind simulations to obtain the required solar wind density profiles and combining it with STEREO and SOHO white light images, the best current techniques are able to predict the arrival times of these shocks with an error bar of no more than a few hours, 1 or 3 days in advance.

Current research is focusing on an interesting subclass of interplanetary shocks that are radio loud near the Sun – that is they produce a well-discernible type II

radio emission – but result in no observable solar wind compressions in near-Earth, in situ measurements. It is postulated that these shocks somehow have deflected and completely missed Earth (Gopalswamy et al. 2012).

Solar Energetic Particles (SEPs)

CMEs ringing the Earth's magnetosphere are not the only space weather dangers emanating from the Sun. The Sun is also the source of a very wide energy spectrum of energetic particles – called solar energetic particles (SEPs) – ranging from tens of keV to well above 100 MeV. Besides solar flares directly injecting energetic particles onto interplanetary magnetic field lines just above the photosphere of the Sun, interplanetary shocks, discussed in the previous section, produce copious amounts of energetic ions and electrons as they propagate outward. While only the most energetic (~1 GeV) SEPs can reach the surface of the Earth due to the deflection of most charged particles by the protective magnetosphere, they represent a significant danger to astronauts, especially during future deep space missions. Also, SEPs cause havoc in modern satellite microelectronics causing memory bit flips, single-event upsets, and latchups that can significantly harm these components. Due to their near-speed-of-light velocities, SEPs arrive to the vicinity of Earth from the Sun in mere 15–30 min. Thus, viable forecasting schemes rely on remote observations of flares and interplanetary shocks.

Tracking interplanetary shocks in the inner heliosphere has been discussed in the previous section. However, knowing the location and speed of a shock is insufficient to accurately predict SEP production rates. In fact, the precise physical mechanisms involved in SEP generation at shocks are not fully understood. The high time resolution solar wind measurements of the Wind spacecraft have recently resulted in a number of discoveries related to the acceleration of charged particles at interplanetary shocks.

Analytical studies of the behavior of charged particles at solar wind shock discontinuities derived that the most energetic SEPs would have to be generated at shocks with such large jumps in density and magnetic field strength that are very rarely observed. Yet, even moderate-size shocks appear to be capable of producing harmful SEPs. In observing interplanetary shocks at 1 AU, Wind measurements revealed that shocks often are composed of multiple up/down steps or shocklets (see Fig. 8 upper panel). In observing the charged particles concurrently, evidence was found for diffusive shock acceleration (see Fig. 8 lower panel), whereby particles gain energy by traversing a shock ramp multiple times and diffuse in pitch angle and energy by scattering off of upstream and downstream shocklets or large fluctuations (Wilson et al. 2013). This process enables weaker shocks to still produce higher energy particles.

Particularly effective are shock–shock interactions to produce copious amount of energetic particles. Catching the moment of interaction between two extremely fast-moving shocks in interplanetary space is highly unlikely. However, the Wind spacecraft, in cooperation with other near-Earth assets, can readily observe the moments when an interplanetary shock impinges on the Earth's bow shock.

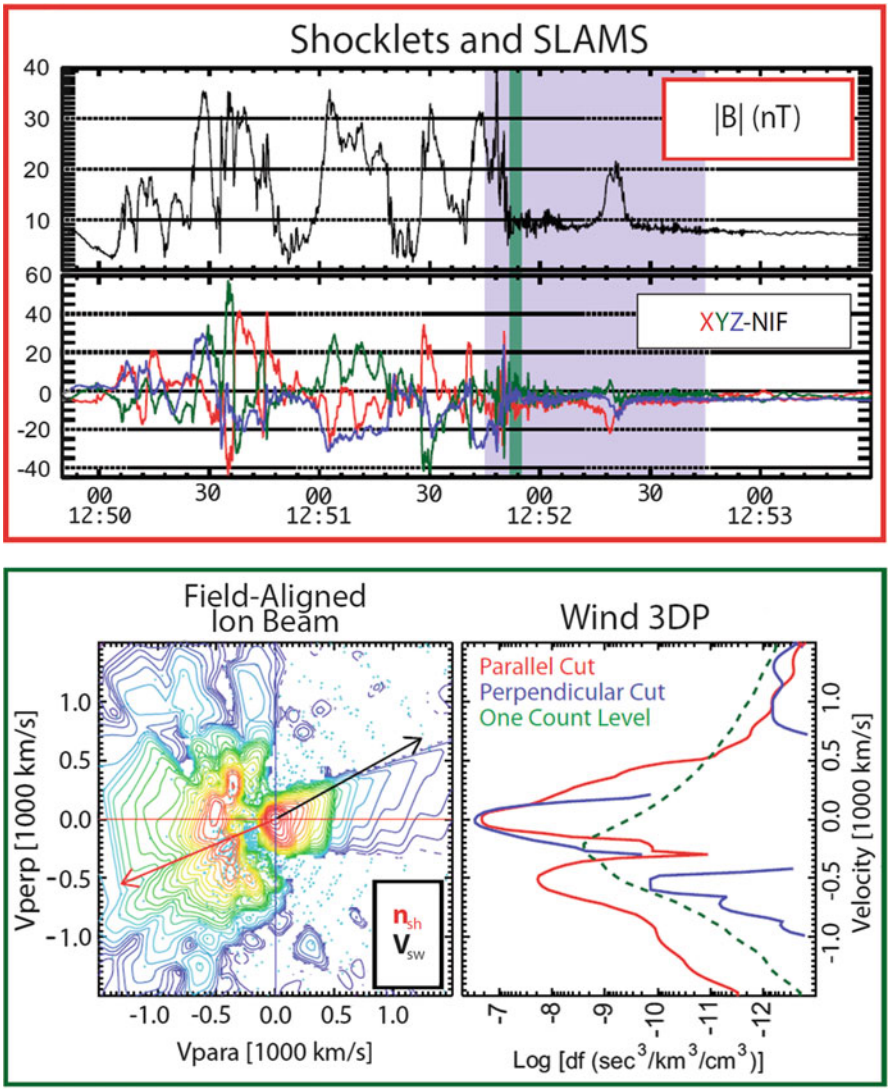

Fig. 8 (*Upper*) Overview of the magnetic field profiles of a series of shocklets and SLAMS observed by Wind/MFI at an interplanetary shock. The *green* shaded region corresponds to the time period for the *lower panel*. (*Lower*) Ion velocity distribution showing contours of constant phase-space density (bulk flow frame) in the plane containing the average magnetic field direction (along the *horizontal*) and the solar wind velocity vector Vsw. *Red* peaks *left* of the plot center show accelerated ions (After Wilson et al. 2013)

It appears that one shock starts the acceleration process of the particles creating a pool of seed population that the second shock further accelerates to the higher energy ranges. In effect, the two shocks as they collide form a magnetic trap that is particularly efficient at accelerating charged particles.

Finally, Wind observations also shed some light on how magnetic reconnection in solar flares accelerates particles. Magnetic reconnection also operates in the 1 AU solar wind, though it is not nearly as energetic of a process as in solar flares. But 1 AU magnetic reconnection is readily observable by the Wind spacecraft. It appears that magnetic field lines do not have to be oriented precisely in the opposite direction in order to reconnect. In fact, component reconnection is much more prevalent than full magnetic cancelation (Gosling 2007). Wind observations also established that electron two-stream instability is the physical mechanism responsible for transferring magnetic energy of the reconnecting field lines to particle acceleration (Malaspina et al. 2013). These Wind observations and results pave the way for future predictive capabilities of SEP generation and forecasting.

Conclusion

Over the past 20 years, the Wind spacecraft has collected valuable observations of the 1 AU solar wind, impinging on the Earth's magnetosphere to advance our space weather prediction capabilities. Making most of its measurements while orbiting the Sun–Earth first Lagrange (L1) point, Wind has been collecting a comprehensive set of solar wind data at an unprecedented time resolution. The mostly multiply redundant instrumentation on the spacecraft has enabled in-depth studies of the structure and evolution of CMEs, interplanetary shock, and of the physical processes of particle acceleration at shocks and magnetic reconnection sites. Moreover, Wind radio wave observation of type II radio bursts generated by interplanetary shocks heading toward Earth has paved the way for future operational space weather forecasting capabilities with multiday lead times. The Wind spacecraft and its complement of instruments are still fully operational with enough fuel to maintain its current L1 orbit for nearly 60 years. Current NASA plans call for many more years of operations of this venerable spacecraft, most assuredly leading to more groundbreaking scientific discoveries.

Cross-References

- ▶ Coronal Mass Ejections
- ▶ Fundamental Aspects of Coronal Mass Ejections
- ▶ Early Solar and Heliophysical Space Missions
- ▶ ISAS-NASA GEOTAIL Satellite (1992)
- ▶ Nature of the Threat/Historical Occurrence
- ▶ Solar and Heliospheric Observatory (SOHO) (1995)
- ▶ STEREO as a "Planetary Hazards" Mission

References

Gopalswamy N, Lara A, Lepping RP, Kaiser ML, Berdichevsky D, St. Cyr OC (2000) Interplanetary acceleration of coronal mass ejections. Geophys Res Lett 27:145–148

Gopalswamy N, MaKela P, Akiyama S, Yashiro S, Xie H, MacDowall RJ, Kaiser ML (2012) Radio-loud CMEs from the disk center lacking shocks at 1 AU. J Geophys Res 117:A08106

Gosling J (2007) Observations of magnetic reconnection in the turbulent high-speed solar wind. Astrophys J Lett 671:L73–L76

Kahler SW, Krucker S, Szabo A (2011) Solar energetic electron probes of magnetic cloud field line lengths. J Geophys Res 116:1104

Malaspina DM, Newman DL, Wilson LB III, Goetz K, Kellogg PJ, Kerstin K (2013) Electrostatic solitary waves in the solar wind: evidence for instability at solar wind current sheets. J Geophys Res 118(2):591–599

Marubashi K (1997) Interplanetary magnetic flux ropes and solar filaments. In: Crooker NU, Joselyn JA, Feynman J (eds) Coronal mass ejections, vol 99, Geophysical monograph. American Geophysical Union, Washington, DC, p 147

Michalek G, Gopalswamy N, Lara A, Manoharan PK (2004) Arrival time of halo coronal mass ejections in the vicinity of the Earth. Astron Astrophys 423:729–736

Möstl C, Farrugia CJ, Kilpua EKJ, Jian LK, Liu Y, Eastwood JP, Harrison RA, Webb DF, Temmer M, Odstrcil D, Davies JA, Rollett T, Luhmann JG, Nitta N, Mulligan T, Jensen EA, Forsyth R, Lavraud B, de Koning CA, Veronig AM, Galvin AB, Zhang TL, Anderson BJ (2012) Multi-point shock and flux rope analysis of multiple interplanetary coronal mass ejections around 2010 August 1 in the inner heliosphere. Astrophys J 758:10. doi:10.1088/0004-637X/758/1/10

Nieves-Chinchilla T, Colaninno R, Vourlidas A, Szabo A, Lepping RP, Boardson SA, Anderson BJ, Korth H (2012) Remote and in-situ observations of an unusual Earth-directed coronal mass ejection from multiple viewpoints. J Geophys Res 117:6106

Odstrcil D, Riley PC, Zhao XP (2004) Numerical simulation of the 12 May 1997 interplanetary CME event. J Geophys Res 109. doi:10.1029/2003JA010135

Wilson LB III, Koval A, Sibeck DG, Szabo A, Cattell CA, Kasper JC, Maruca BA, Pulupa M, Salem CS, Wilber M (2013) Shocklets, SLAMS, and field-aligned ion beams in the terrestrial foreshock. J Geophys Res 118(3):957–966